J. Water Environ. Nanotechnol., 4(1): 31-39 Winter 2019

ORIGINAL RESEARCH PAPER

Novel and ecofriendly synthesis of Ag-TiO_2-G photocatalyst and investigate the effect of graphene in photodegradation of an organic pollutant in water

Farnosh Tavakoli, Alireza Badiei*, Jahan Bakhsh Ghasemi

School of Chemistry, College of Science, University of Tehran, Tehran, Iran

Received: 2018-08-15 Accepted: 2018-12-04 Published: 2019-02-01

ABSTRACT

In this paper, Ag-TiO_2-Graphene (Ag-TiO_2-G) photocatalyst is synthesized via an economic and green rout. Pranus Cerasus is applied as a green reducing agent due to the presence of anthocyanin pigment. The anthocyanin molecules are responsible for the red color of the prunus cerasus seeds. The nanocomposites were characterized by XRD, EDS mapping, DRS and TEM. In order to explore the presence of Ag, different mass ratio of Ag to in Ag-TiO_2-G composite (5wt%, 10wt%, 15wt%, 20wt%, 25wt%, 30wt%, 35wt%, 40wt%, 45wt%, and 50wt%) were synthesized and their performance on the Acid Orange 7 (AO7) photodegradation were compared with bare graphene. In addition, for investigation of the presence of graphene, the Ag-TiO_2 was synthesized and compared with the Ag-TiO_2-G composite from the photocatalytic performance point of view. Ag nanoparticles and graphene are two crucial factors in AO7 photodegradation. Finally, we showed that photodegradation of AO7 with photocatalyst depends on photogenerated holes.

Keywords: *Ag-TiO_2-G; AO7; Green Synthesis; Photocatalyst; Pranus Cerasus*

How to cite this article

Tavakoli F, Badiei A, Ghasemi BJ. Novel and ecofriendly synthesis of Ag-TiO_2-G photocatalyst and investigate the effect of graphene in photodegradation of an organic pollutant in water. J. Water Environ. Nanotechnol., 2019; 4(1): 31-39.
DOI: 10.22090/jwent.2019.01.003

INTRODUCTION

Pollution of water has become a dilemma in recent years. So, researchers are interested to find a way to eliminate pollution from wastewater and reuse it. For degradation of the organic pollutants, graphene-based photocatalysts are effective agents [1-3]. On the other hands, silver nanoparticles have excellent photocatalytic properties for the elimination of the water pollutants [4, 5]. The placement of silver nanoparticles on the graphene improves the photocatalytic properties of these nanoparticles due to the superior electron mobility and high specific surface area of graphene [6-8].

Graphene is a material with extraordinary properties [9, 10]. It should be noted that the nanoparticles are directly decorated on the graphene sheets without any molecular linkers. Therefore, many types of nanoparticles can be deposited on the graphene sheets and create interesting applications such as catalytic, energy storage, photocatalytic, and optoelectronic applications [11]. There are various methods for synthesis graphene composites, includes pre-graphitization, post-graphenization and syn-graphenization [12, 13].

The TiO_2 nanoparticles have been used for photocatalytic elimination of dyes due to their extraordinary optical properties [14-16]. The photocatalytic degradation mechanism of TiO_2 nanoparticles has been proven [17, 18]. One of the TiO_2 problems is the recombination of electrons and holes [19]. But, graphene can solve this problem of TiO_2 due to its amazing electron mobility and large surface area. On the other hand, graphene can act as an efficient transmitter and acceptor electron to improve photoinduced charge

* Corresponding Author Email: *abadiei@khayam.ut.ac.ir*

transfer, therefore, it can inhibit the recombination of the photogenerated electron-holes [20].

In recent years, for the synthesis of nanomaterials, researchers have preferred the use of natural ingredients instead of chemicals. So they used natural fruits or vegetables instead of hazardous chemicals reagents [21]. Here, for the first time, we used prunus cerasus juice as a natural reducing agent to synthesize Ag-G. The reductant property of prunus cerasus is due to anthocyanins. They are responsible for the color of the prunus cerasus seeds. Six anthocyanins have been described in this fruit: 3,5 diglycoside derivatives and 3delphinidin, cyaniding and pelargonidin glycosides. Antioxidant properties of prunus cerasus induce also by a phenolic compound such as anthocyanins. This work demonstrates a green and economical method for the preparation of Ag-TiO_2-G. Prunus cerasus juice is a rich source of anthocyanine. The photocatalytic performance of Ag-TiO_2-G was investigated for photodegradation of acid orange 7 (AO7) as a pollutant compound model. In order to check the presence of Ag metal in photodegradation performance of AO7, bare graphene was tested in the photodegradation of AO7. On the other hands, the weight ratio of Ag in graphene was investigated as a crucial effect on photodegradation performance.

EXPERIMENTAL

Synthesis of Ag-TiO_2-G

All the reagents for the synthesis of Ag-TiO_2-G were commercially available from Merck and employed without any further purification. The prunus cerasus was obtained from Shiraz in Iran. Ag-TiO_2-G nanostructures were prepared by the following experimental sequence: first, a certain amount of silver nitrate and 0.2 gr TiO_2 was added dropwise into the graphene oxide solution (2gr of graphene oxide dispersed in 50 mL of distilled water) that was synthesis via Hummer method [22] under ultrasonic irradiation, and then 50ml Pranus Cerasus was added dropwise into the above solution. The obtained mixture was stirred at room temperature for 12h. The resultant precipitates were filtered, washed with distilled water and absolute ethanol and dried at 60°C in a vacuum. Finally, the product was treated at 450°C under Ar gas. Synthesis procedure of Ag-TiO_2-G is shown schematically in Fig. 1. The experiment was carried out by using 5wt%, 10wt%, 15wt%, 20wt%, 25wt%, 30wt%, 35wt%, 40wt%, 45wt% and 50wt% of Ag in Ag-TiO_2-G composite at the same conditions.

Synthesis of Ag-TiO_2

Ag-TiO_2 nanostructures were prepared by the following experimental sequence: first, a certain amount of silver nitrate was added dropwise into the TiO_2 solution (2gr of TiO_2 dispersed in 50 mL of distilled water) under ultrasonic irradiation, and then 50ml Pranus Cerasus was added dropwise into the above solution. The obtained mixture was stirred at room temperature for 12h. The resultant precipitates were filtered, washed with distilled water and absolute ethanol and dried at 60°C in a vacuum. Finally, the product was treated at 450°C under Ar gas. The experiment was carried out

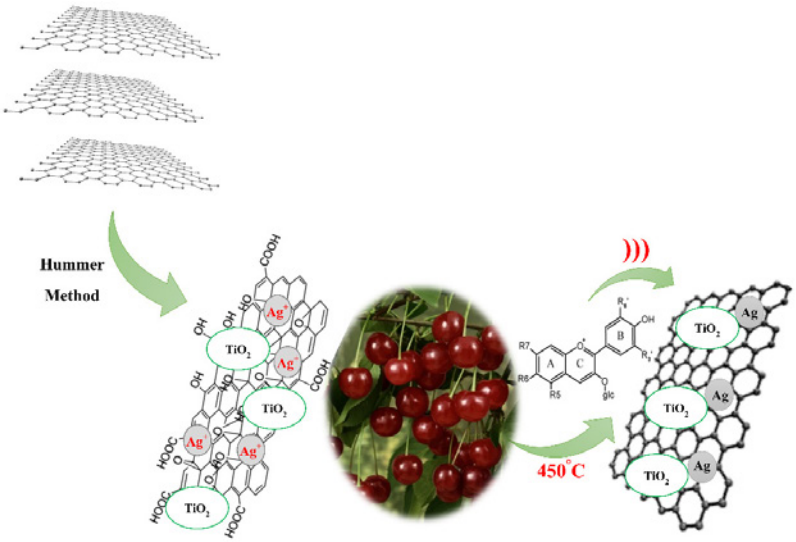

Fig. 1. Green synthesis procedure of Ag-TiO_2-G via Pranus Cerasus.

by using 5wt%, 10wt%, 15wt%, 20wt%, 25wt%, 30wt%, 35wt%, 40wt%, 45wt% and 50wt% of Ag to TiO_2 at the same conditions, respectively.

Photocatalytic Degradation Experiment

8W (UV-C) mercury lamp (Philips, Holland) emitting around 254 nm, positioned on top of the batch quartz reactor was used for degradation processes.

RESULTS AND DISCUSSION

Fig. 2(a-d) shows the XRD pattern of graphene oxide, TiO_2, Ag-TiO_2-G, and Ag-G. The diffractogram of graphene oxide exhibited the typical reflections at 2θ = 26.48° and 43.17° corresponding to the (002) and (100) reflections (JCPDS 01-0646) (Fig. 2a). According to Fig. 2b for the TiO_2 compound, the XRD reflections at 2θ of 25.8°, 38°, 39.5°, 48°, 55°, 62.6°, 69.7°, and 75.7° can be indexed to the characteristic reflections of the (101), (004), (112), (200), (211), (213), (220) and (215) plane reflections of anatase crystal structure TiO_2 respectively. According to Fig. 2c For the Ag-TiO_2-G compound, the XRD reflections at 2θ of 27.1°, 38.4°, 42.8°, and 64.2° can be indexed to the characteristic reflections of the (002), (111), (200) and (220) plane reflections. The reflections at 2θ of 38.4°, 42.8°, and 64.2° are due to the presence of Ag on the surface of graphene sheets (Fig. 2d). The (002) reflection of graphene oxide overlapped the (002) reflection of Ag-TiO_2-G compound. On the other hand, for the Ag-TiO_2-G composite, the (002) and (100) reflection of graphene overlapped the anatase (200) and (113) reflection of TiO_2.

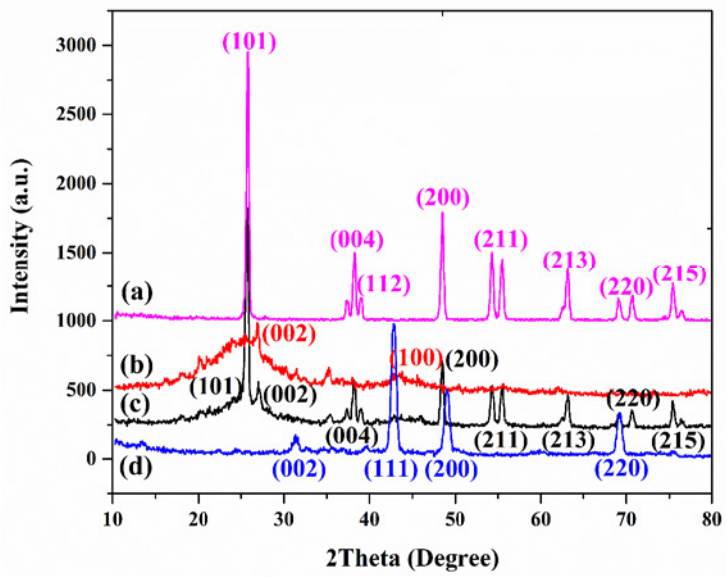

Fig. 2. XRD patterns of (a) graphene oxide, (b) TiO_2, (c) Ag-TiO_2-G and (d) Ag-G compounds.

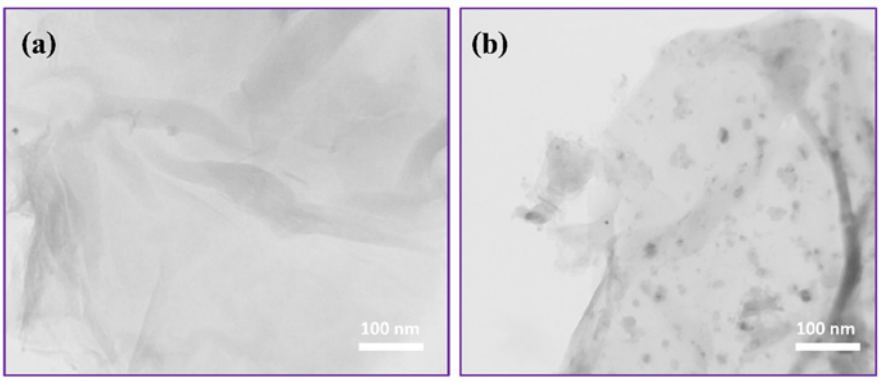

Fig. 3. TEM images of (a) graphene and (b) Ag-TiO_2-G.

Fig. 3(a, b) shows the TEM images of Ag-TiO_2-G and graphene oxide. According to TEM image, Ag and TiO_2 nanoparticles are well distributed on graphene sheets. As shown in TEM images the particle size of Ag and TiO_2 nanoparticles are (10-20) nm and (30-40) nm respectively and the graphene that was synthesis is one layer.

To get information on the elements, the Ag-TiO_2-G compound was examined by EDX analysis. Fig. 4 shows the EDX analysis of the Ag-TiO_2-G composite. In the EDX spectrum of Ag-TiO_2-G composite, the main elements such as Ag, Ti, O, and C were presented. According to EDX analysis, Ag and TiO_2 nanoparticles are well placed on the graphene surface.

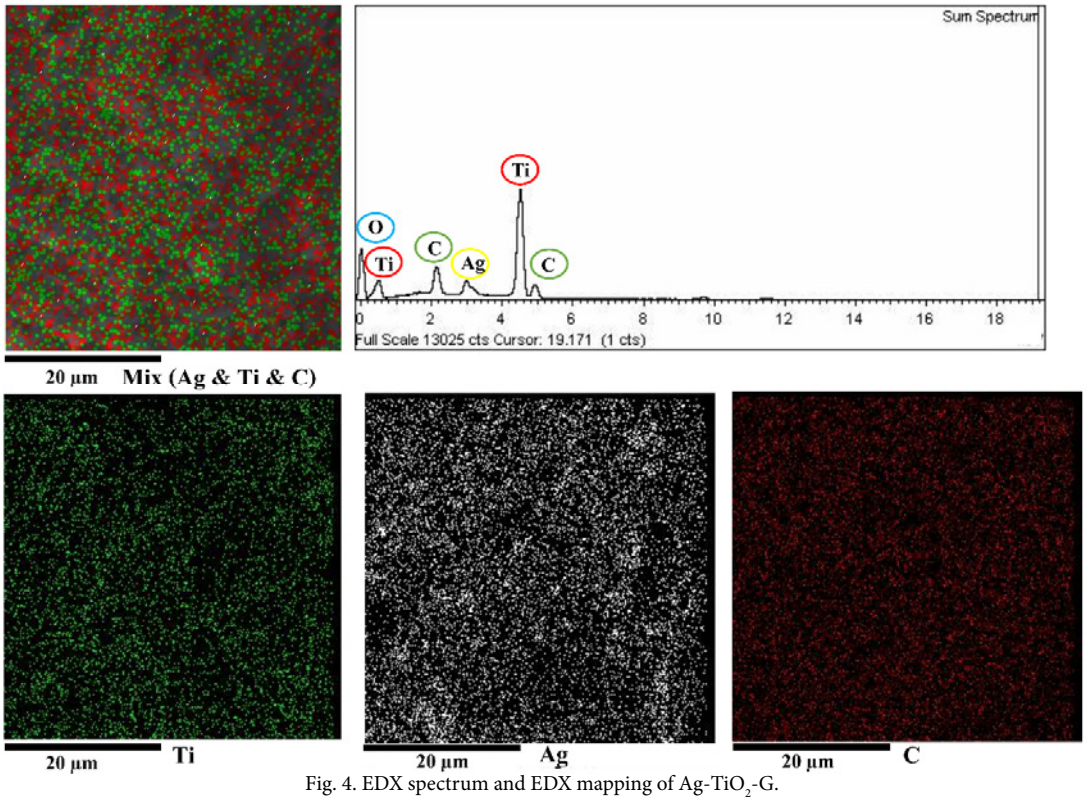

Fig. 4. EDX spectrum and EDX mapping of Ag-TiO_2-G.

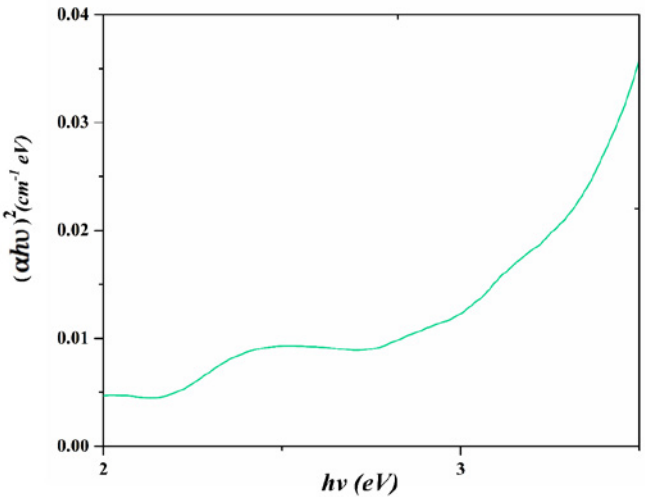

Fig. 5. Diffuse Reflectance Spectra (DRS) of Ag-$TiO_{2\text{-}G}$.

Fig. 5 shows the DRS spectrum of Ag-TiO_2-G composite. According to our recent paper, the band gap of TiO_2 was 3.24 eV [23]. The calculated bandgap energies Ag-TiO_2-G is 2.57 eV. The slightly reduced bandgap of Ag-TiO_2-G composite implies that unpaired π electrons from graphene may bond with free electrons of TiO_2.

UV-visible diffused reflectance spectra of TiO_2 and Ag-TiO_2 were shown in Fig. 6. Compared with an absorption edge of TiO_2 which was detected at around 387nm, a red shift to the higher wavelength at 447nm in the absorption edge of the Ag-TiO_2 compound could be observed. It means that the Ag-TiO_2 catalyst underwent a redshift of about 110nm. So the calculated band gap of Ag-TiO_2 is about 2.77. Based on results narrowing the band gap of TiO_2 is due to the Ti-O-Ag bonds. Electrons flow from the higher to lower Fermi level to adjust the Fermi energy levels. The calculated conduction band position of anatase TiO_2 is about -4.21 eV

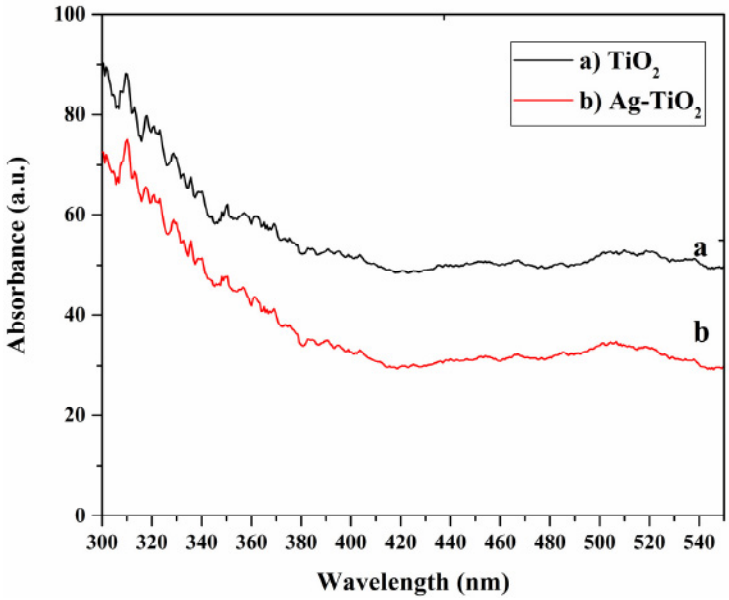

Fig. 6. Diffuse Reflectance Spectra (DRS) of TiO_2 and $_{Ag-}TiO_{2.}$

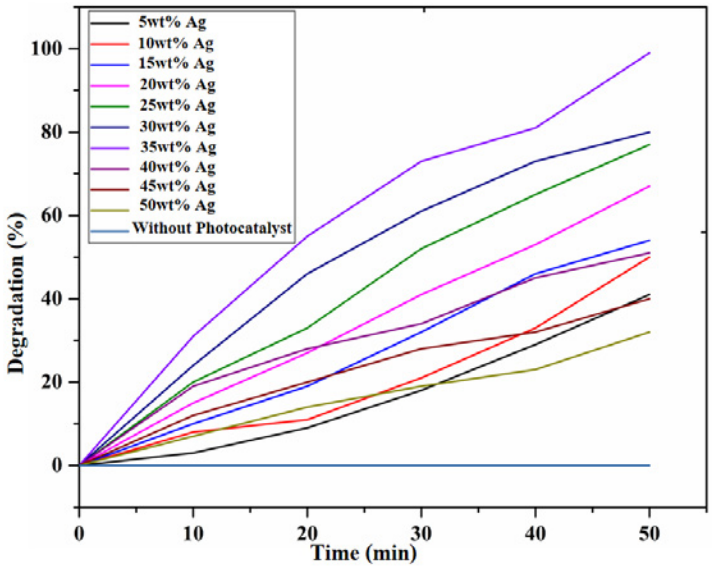

Fig. 7. Degradation curve of AO7 aqueous dye with UV light without photocatalyst and different weight ratio of Ag in Ag-$TiO_{2.}$G composite.

Table 1. Investigation the effect of graphene in degradation efficiency of AO7

Samples	Weight ratio of Ag in ($Ag-TiO_2$)	DE% of ($Ag-TiO_2$)	Weight ratio of Ag in ($Ag-TiO_2$-G)	DE% of ($Ag-TiO_2$-G)
1	5wt%	22%	5wt%	41%
2	10wt%	32%	10wt%	50%
3	15wt%	39%	15wt%	54%
4	20wt%	41%	20wt%	67%
5	25wt%	49%	25wt%	77%
6	30wt%	54%	30wt%	80%
7	35wt%	76%	35wt%	99%
8	40wt%	42%	40wt%	51%
9	45wt%	29%	45wt%	40%
10	50wt%	18%	50wt%	32%

DE: Degradation Efficiency

with a band gap of about 3.2 eV, silver can accept the photoexcited electrons from TiO_2. So, electron-hole recombination is reduced.

Photocatalytic performance of Ag-TiO_2-G compounds

The photocatalytic performance of the Ag-TiO_2-G and bare graphene were investigated using aqueous AO7 dye as a model compound. As shown in Fig. 7, when only AO7 dye was exposed to UV light, no degradation of AO7 was observed. Only the photocatalyst is responsible for degradation of AO7. To investigate the effect of Ag loading, the different weight ratio of Ag (5wt%, 10wt%, 15wt%, 20wt%, 25wt%, 30wt%, 35wt%, 40wt%, 45wt%, and 50wt%) loaded on graphene were prepared and then tested (Fig. 7). The sample with 35wt% Ag showed higher photocatalytic degradation compared to bare graphene nanoparticles, while 5wt% and 50wt% Ag loaded graphene, the photocatalytic activity was decreased. As shown in Fig. 7, with increasing the weight ratio of Ag to graphene, the photocatalytic performance of coupled nanoparticles was decreased, decreasing the photodegradation is due to the higher loading of Ag that increase the recombination rate of electrons and holes and so prevented the separation of charges. The second reason is that higher loading of Ag may decrease the surface area of graphene and absorptivity of coupled nanoparticles for adsorbed dye molecules on the surface of graphene and thereby influence the photocatalytic performance and so prevented the reaching light to active sites of the compound. It can be seen in Fig. 7 that graphene with 35wt% Ag exhibits 99% AO7 degradation within 20 min but only 61% of degradation was shown in the presence of bare TiO_2. Generally, to investigate the photocatalytic performance of Ag-TiO_2-G nanocomposite, several samples with a different weight ratio of Ag to graphene were synthesized. According to Fig. 7, with increasing the weight ratio of Ag from 5 wt% to 10 wt%, 15 wt%, 20 wt%, 25 wt%, 30wt% and 35wt% photodegradation was increased from 41% to 50%, 54%, 67%, 77%, 80% and 99% respectively. But with increasing the weight ratio of Ag from 35 wt% to 40wt%, 45wt%, and 50 wt%, photodegradation was decreased from 99% to 51%, 40% and 32% respectively.

Effect of graphene in photocatalytic performance

The photocatalytic performance of the Ag-TiO_2 was investigated using aqueous AO7 dye as a model compound under UV light irradiation and compared with graphene loaded Ag-TiO_2 samples to investigate the effect of graphene. All the Ag-TiO_2 samples were compared with graphene loaded composite samples corresponding to themselves.

As shown in Table 1, different weight ratio of Ag (5wt%, 10wt%, 15wt%, 20wt%, 25wt%, 30wt%, 35wt%, 40wt%, 45wt%, and 50wt%) loaded on TiO_2 photocatalyst was prepared, then

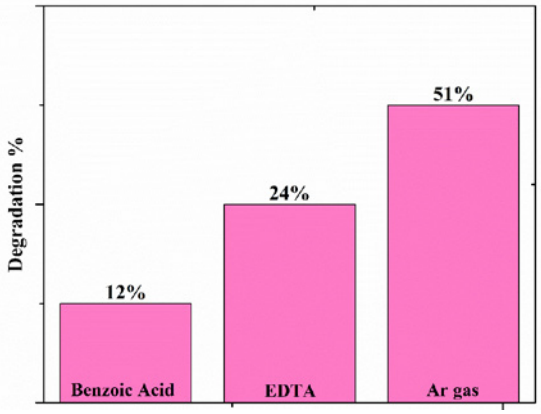

Fig. 8. A series of trapping experiments (a) Benzoic Acid, (b) EDTA and (c) Ar gas for the degradation of AO7 over Ag-TiO_2-G photocatalysts under UV light irradiation.

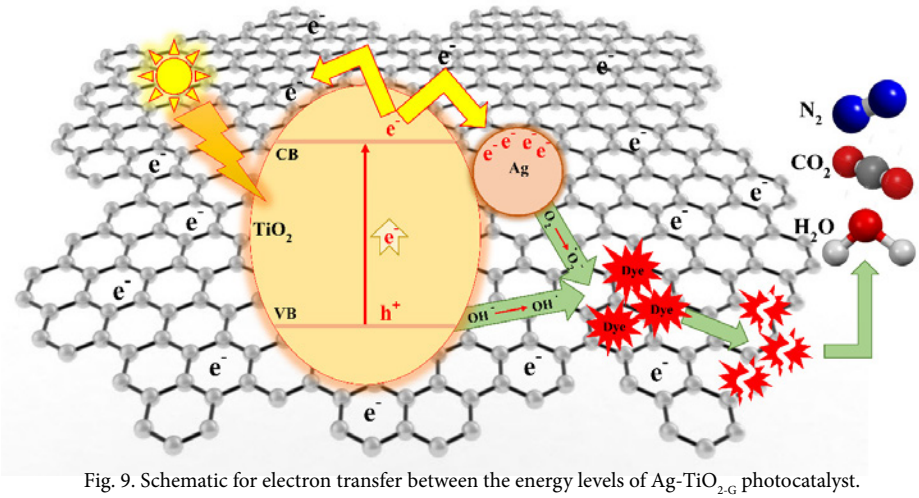

Fig. 9. Schematic for electron transfer between the energy levels of Ag-$TiO_{2\text{-}G}$ photocatalyst.

their photocatalytic performance was tested and also compared with their corresponding graphene loaded samples. According to Table 1, two composites (Ag-TiO_2 and Ag-TiO_2-G) were compared for photocatalytic performance in the presence and absence of graphene. Based on the results, graphene has a crucial effect in the photodegradation of pollutants due to its superior properties such as large surface area, electron mobility and create Delays in recombination of electrons and holes.

Effect of graphene on degradation time

Based on the results, graphene had a crucial effect on the degradation of organic pollutant in water. The graphene loaded Ag-TiO_2 compound not only increased degradation efficiency but also decreased the degradation time. Decreasing the degradation time of AO7 caused by high adsorption ability of graphene in Ag-TiO_2-G compound. In comparison with Ag-TiO_2 that degraded the AO7 in 50 min, Ag-TiO_2-G degraded the AO7 in 20 min.

Mechanism of photodegradation of AO7

During photocatalysis, hydroxyl radicals, superoxide anions (O2-.) and holes (h+) are the reactive species. In order to understand the photocatalytic activity of Ag-G compound for the degradation of AO7, a series of free radicals trapping experiments were carried out, as shown in Fig. 8. In the presence of hydroxyl radicals scavenger such as benzoic acid (0.5mM), 12% degradation was observed. In the case of benzoic acid, 87% degradation was decreased than that of the scavenger-free photocatalytic system for AO7, as shown in Fig. 8. To examine the exact reactive species that are involved in AO7 degradation, 10ml EDTA (0.01M), as an effective h+ scavenger was added into the AO7 reaction solution. The rate of AO7 degradation was drastically suppressed, i.e. only 24% of AO7 degradation was noticed (Fig. 8b). This results confirmed that the photoinduced holes and hydroxyl radicals are crucial agents in the degradation of AO7. Another experiment was performed under Ar atmosphere as shown in Fig. 8c. A high purity Ar gas was continuously purged throughout the reaction process under an ambient condition which eliminates the dissolved oxygen content from the reaction solution and thereby prevents the formation of O_2-•. As a result, 51% in AO7 degradation was observed after 20 min of UV light illumination instead of 99% in a normal atmospheric condition. These results clearly emphasized that AO7 degradation mainly depends on photogenerated holes and hydroxyl radicals.

Fig. 9 shows the electron transfer between the energy levels of titanium dioxide, silver and graphene. Based on Fig. 9, when the light reaches the titanium dioxide particles, the electron is transferred from the valence band to the conduction band of TiO_2. Then, silver nanoparticles act as an electron acceptor and accept electrons from the TiO_2 conduction level. On the other hands, electrons can transfer to the electrons that are a presence on the surface of graphene. According to the results, the recombination of electrons and holes was prevented.

As shown in Fig. 9, the oxygen molecules reacted with the electrons of the conduction band and created the O_2-•. On the other hands, the hydroxyl ions those are adsorbed on the surface of photocatalyst reacted with the positive ions in the valence band and created the hydroxyl radicals. Hydroxyl radicals are high reactive species those are responsible for degradation of AO7 dyes. As shown in Fig. 9, when AO7 dye degraded the CO_2, H_2O molecules and N_2 gas were formed.

CONCLUSION

Ag-TiO_2-G compound was prepared by pranus cerasus as a green reducing agent. The as-produced were characterized by using XRD, TEM, FESEM, EDS, and DRS. Ag-TiO_2-G compound with 30wt% Ag showed higher photocatalytic performance in the photodegradation of AO7 than pure TiO_2, bare graphene, and Ag-TiO_2 compound. In order to investigate the presence of graphene, different weight ratio of Ag (5wt%, 10wt%, 15wt%, 20wt%, 25wt%, 30wt%, 35wt%, 40wt%, 45wt%, and 50wt%) in the composite of Ag-TiO_2-G were synthesized and their performance in AO7 photodegradation were compared with the corresponding samples without graphene. The results show that the significant enhancement in the photodegradation efficiency for the degradation of AO7 was due to the presence of Ag metal and graphene, which possesses effective charge carrier separation properties and high surface area.

ACKNOWLEDGMENT

Authors are grateful to the Council of the University of Tehran for providing financial support to undertake this work.

CONFLICT OF INTEREST

The authors declare that there are no conflicts of interest regarding the publication of this manuscript.

REFERENCES

1. Shiravand G, Badiei A, Ziarani GM, Jafarabadi M, Hamzehloo M. Photocatalytic Synthesis of Phenol by Direct Hydroxylation of Benzene by a Modified Nanoporous Silica (LUS-1) under Sunlight. Chinese Journal of Catalysis. 2012;33(7-8):1347-53.
2. Eskandarloo H, Badiei A, Behnajady MA, Ziarani GM. Ultrasonic-assisted degradation of phenazopyridine with a combination of Sm-doped ZnO nanoparticles and inorganic oxidants. Ultrasonics Sonochemistry. 2016;28:169-77.
3. Eskandarloo H, Badiei A, Behnajady MA, Tavakoli A, Ziarani GM. Ultrasonic-assisted synthesis of Ce doped cubic–hexagonal ZnTiO3 with highly efficient sonocatalytic activity. Ultrasonics Sonochemistry. 2016;29:258-69.
4. Fujishima A, Zhang X, Tryk D. TiO2 photocatalysis and related surface phenomena. Surface Science Reports. 2008;63(12):515-82.
5. Hashimoto K, Irie H, Fujishima A. TiO2Photocatalysis: A Historical Overview and Future Prospects. Japanese Journal of Applied Physics. 2005;44(12):8269-85.
6. Malato S, Fernández-Ibáñez P, Maldonado MI, Blanco J, Gernjak W. Decontamination and disinfection of water by solar photocatalysis: Recent overview and trends. Catalysis Today. 2009;147(1):1-59.
7. Tavakoli F, Salavati-Niasari M, Mohandes F. Green synthesis of flower-like CuI microstructures composed of trigonal nanostructures using pomegranate juice. Materials Letters. 2013;100:133-6.
8. Eskandarloo H, Badiei A, Haug C. Enhanced photocatalytic degradation of an azo textile dye by using TiO2/NiO coupled nanoparticles: Optimization of synthesis and operational key factors. Materials Science in Semiconductor Processing. 2014;27:240-53.
9. Shen J, Hu Y, Shi M, Li N, Ma H, Ye M. One Step Synthesis of Graphene Oxide−Magnetic Nanoparticle Composite. The Journal of Physical Chemistry C. 2010;114(3):1498-503.
10. Geim AK, Novoselov KS. The rise of graphene. Nature Materials. 2007;6(3):183-91.
11. Singh V, Joung D, Zhai L, Das S, Khondaker SI, Seal S. Graphene based materials: Past, present and future. Progress in Materials Science. 2011;56(8):1178-271.
12. Tavakoli F, Salavati-Niasari M. A facile synthesis of CuI-graphene nanocomposite by glucose as a green capping agent and reductant. Journal of Industrial and Engineering Chemistry. 2014;20(5):3170-4.
13. Salavati-Niasari M, Tavakoli F. Pb(OH)I-graphene composite: Synthesis and characterization. Journal of Industrial and Engineering Chemistry. 2015;21:1208-13.
14. Tavakoli F, Salavati-niasari M, Mohandes F. Graphite Nanosheets: Thermal Treatment Synthesis and Characterization. Synthesis and Reactivity in Inorganic, Metal-Organic, and Nano-Metal Chemistry. 2015;46(6):877-82.
15. Eskandarloo H, Badiei A, Behnajady MA, Ziarani GM. Ultrasonic-assisted degradation of phenazopyridine with a combination of Sm-doped ZnO nanoparticles and inorganic oxidants. Ultrasonics Sonochemistry. 2016;28:169-77.
16. Eskandarloo H, Badiei A, Behnajady MA, Tavakoli A, Ziarani GM. Ultrasonic-assisted synthesis of Ce doped cubic–hexagonal ZnTiO3 with highly efficient sonocatalytic activity. Ultrasonics Sonochemistry. 2016;29:258-69.
17. Fujishima A, Zhang X, Tryk D. TiO2 photocatalysis and related surface phenomena. Surface Science Reports. 2008;63(12):515-82.
18. Hashimoto K, Irie H, Fujishima A. TiO2Photocatalysis: A Historical Overview and Future Prospects. Japanese Journal of Applied Physics. 2005;44(12):8269-85.
19. Malato S, Fernández-Ibáñez P, Maldonado MI, Blanco J, Gernjak W. Decontamination and disinfection of water by solar photocatalysis: Recent overview and trends. Catalysis Today. 2009;147(1):1-59.
20. Escobedo S, Serrano B, Calzada A, Moreira J, de Lasa H. Hydrogen production using a platinum modified TiO 2 photocatalyst and an organic scavenger. Kinetic modeling. Fuel. 2016;181:438-49.

21. Huang Q, Tian S, Zeng D, Wang X, Song W, Li Y, et al. Enhanced Photocatalytic Activity of Chemically Bonded TiO2/Graphene Composites Based on the Effective Interfacial Charge Transfer through the C–Ti Bond. ACS Catalysis. 2013;3(7):1477-85.
22. Tavakoli F, Badiei A, Yazdian F, Ziarani GM, Ghasemi J. Optimization of Influential Factors on the Photocatalytic Performance of TiO2–Graphene Composite in Degradation of an Organic Dye by RSM Methodology. Journal of Cluster Science. 2017;28(5):2979-95.
23. Eskandarloo H, Badiei A, Behnajady MA, Tavakoli A, Ziarani GM. Ultrasonic-assisted synthesis of Ce doped cubic–hexagonal ZnTiO3 with highly efficient sonocatalytic activity. Ultrasonics Sonochemistry. 2016;29:258-69.